ORAL REFERENCE: ICF100125OR

RESIDUAL STRESS EFFECTS ON FATIGUE CRACK PROPAGATION IN FRICTION STIR WELDS

Claudio Dalle Donne and Gilles Raimbeaux

German Aerospace Center, Institute of Materials Research, D-51170 Cologne, Germany

ABSTRACT

Fatigue crack propagation (FCP) tests of 4mm thick friction stir welded (FSW) joints of the aluminum alloys 6013-T6 and 2024-T3 were carried out with compact tension specimens at different mean stress levels (R-ratios) and crack orientations. The da/dN-K curves of the welded specimens are correctly predicted using a simple approach based on the parent material da/dN-K_{eff} data and the residual stress intensity factor distribution obtained from the cut compliance technique. It is concluded that the differences in the FCP behavior were almost completely caused by residual stresses and not by the different resistance of parent and weld material to FCP.

KEYWORDS

Friction stir welding, fatigue crack propagation, residual stresses, cut compliance technique, effective stress intensity factor

INTRODUCTION

Friction stir welding (FSW) is a relatively new process patented by TWI (Cambridge, UK) in 1992 [1]. A friction stir butt weld is produced by plunging a rotating tool into the facing surfaces of the two plates, Figure 1. The tool consists of a shoulder and a profiled pin emerging from it. As the rotating pin moves along the weld line, the material is heated up by the friction generated by the shoulder and stirred by the rotating pin in a process similar to an extrusion. Since the temperatures are well below the melting point, problems associated with the liquid/solid phase transformation are avoided. This allows high quality joining of materials that have been traditionally troublesome to weld conventionally without distortion, cracks or voids such as high strength aerospace aluminum alloys like 2024 or 7475.

Currently, a very limited amount of data on fatigue crack propagation (FCP) in friction stir welded joints exists [2-4], even though the FCP behavior of long cracks under defined environment is one of the key issues during the material selections for light weight aerospace structures. Most of the work on fatigue of aluminum friction stir welds has been restricted to the generation of S-N data [4-7].

Preliminary FCP experiments with welded specimens of the aluminum alloys 2024-T3 [3] and 6013-T6 [4] displayed lower crack growth rates in the weld than in the base material, especially in the range of low crack propagation rates and stress ratios. It has been suggested that increased resistance against FCP is connected to the fine grained material in the weld [2] or to compressive welding stresses in the compact tension

specimens used in the FCP investigations [3, 4]. The objective of this paper is to examine the influence of residual stresses on the fatigue crack propagation curves of friction stir welded joints in 2024-T3 and 6013-T6 aluminum alloys.

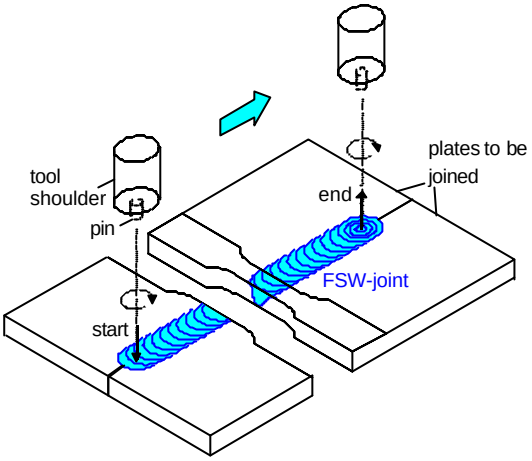

Figure 1: Schematic of friction stir butt welding

EXPERIMENTAL PROCEDURE

Materials and Friction Stir Welding

Two types of 4 mm thick aluminum alloy sheets, 2024-T3 and 6013-T6, were welded on conventional milling machines at DLR and EADS Corporate Research Center on the basis of the TWI patent. The welding direction was always in rolling direction. The ultimate tensile strength values of the joints were in the range of 90 % (2024-T3) and 80 % (6013-T6) of the parent material's ultimate strength. Further details such as process parameters, microstructures, hardness distributions and strength values are found in [4, 5, 8].

FCP tests

The test were carried out with 50 mm wide compact tension specimens at different mean stress levels (R-ratios) and crack orientations, Figure 2. The negative load ratio curves of the 6013-T6 base material were obtained from 80 mm wide middle cracked tension specimens (M(T)). All tests with FSW specimens were performed in the "as-welded" condition.

The "longitudinal weld" LW specimens had cracks in the center of the weld propagating parallel to the welding direction. On these specimens constant amplitude da/dN-K tests were carried out at room temperature and in laboratory air on a computer controlled servo-hydraulic testing machine following ASTM E 647 [9]. In the "transverse weld" TW specimens the crack approached the weld perpendicularly. These tests were carried out only with 6013-T6 FSW joints at constant K-values. In parent material specimens this procedure would have led to constant crack propagation rates. Therefore differences and changes in da/dN of the TW-specimens can be directly attributed to residual stresses or changes in microstructure. Crack propagation was always monitored through the potential drop technique.

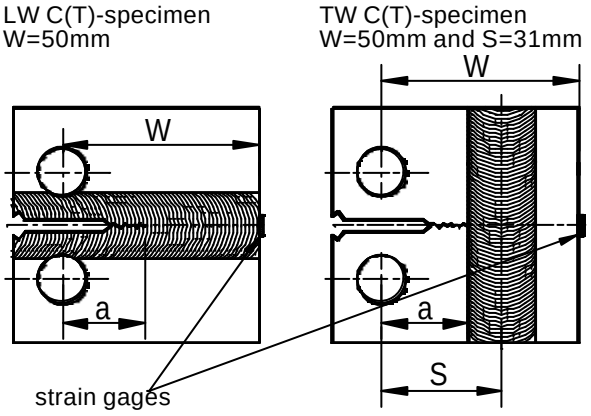

Figure 2: Welded specimen configurations.

Residual stress intensity factor measurement

The stress intensity factor due to residual stresses K_{rs} was determined directly with the so called "cut compliance method" [10, 11]. The method is based on the crack compliance method: a narrow saw cut is introduced progressively in the potential crack plane of the considered specimen or component and the resulting strain change is measured by a strain gauge. The desired stress intensity factor is proportional to the slope of the measured strain plotted as a function of the depth of the cut (i. e. crack length a):

$$K_{rs} = \frac{E'}{Z(a)}\frac{d\varepsilon}{da} \qquad Z(a) = -\frac{2.532}{(W-a)^{1.5}}\left(1 - e^{-6.694\frac{a}{W}}\right) \qquad (1)$$

The proportionality factor or influence function Z(a) is a unique function, that depends only on the cut depth, the geometry of the specimen or component and the strain measurement location. In this investigation a strain gage was glued on the C(T) specimen at the location indicated in Figure 2. The influence function for the set-up was obtained by a fit of the finite element results of Schindler [12] also given in eqn. (1).

Besides its simplicity, the great advantage of this method is that it delivers the information about residual stresses in a suitable form for direct use in fracture mechanics. Moreover the elastic re-distribution of residual stresses with increasing crack or slit length is already included in the K_{rs} versus a/W solution.

Figure 3 shows the distribution of K_{rs} measured by introducing an 0.3 mm wide fret saw cut in the ligament of the welded C(T) specimens. Mean values of at least 2 cutting test were used for one curve. The measured strain versus cut depth (a) data of the LW specimens were fitted by third to fifth degree polynomials, whereas a 12 degree polynomial was employed for the -a-relationship of the TW specimen.

The negative stress intensity factors of Figure 3 are related to compressive residual stresses ahead of the crack. In the longitudinal weld specimens, the residual stresses re-arrange after a crack growth increment in such way that compressive stresses are maintained at the crack tip. With increasing crack length the magnitude of the compressive residual stresses decreases and finally only small amounts of tensile stresses are active at the tips of long cracks. Such a behavior was also observed in C(T) specimens cut out from gas metal arc welded steel plates [13].

Cutting of TW-specimens out of the 6013-T6 plates resulted also in compressive residual stresses ahead of the crack, Figure 3 right side. The residual stresses are however higher in magnitude than in the longitudinal weld case and two peaks are reached in the heat affected zones of the weld.

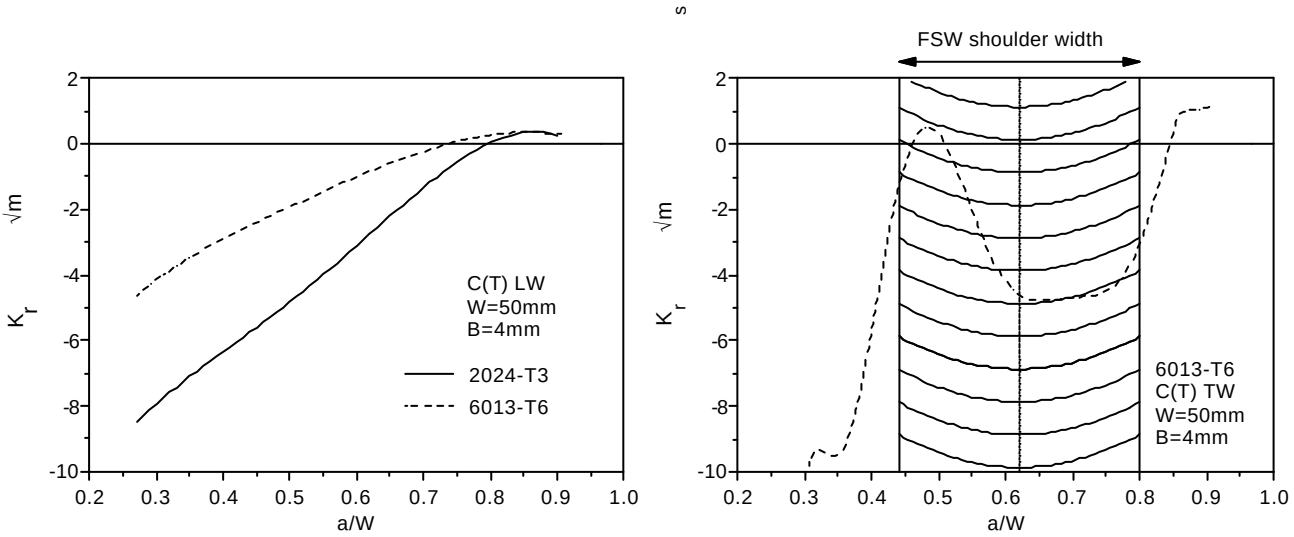

Figure 3: Distribution of the stress intensity factor due to residual stresses in the ligament of the C(T) specimens (left: longitudinal weld specimen, right: transverse weld specimen).

FCP IN LONGITUDINAL WELD SPECIMENS

In Figure 4 the da/dN-K curves of longitudinal weld specimens (closed symbols) are compared to the base material curves (open symbols). At high mean stress levels or R-ratios there is no difference in the FCP behavior of parent material and welded joint. At low R-ratios and loads (R = 0.1, K < 15 MPa√m) there is however an apparent improvement of the welded material properties in both alloys. It is now demonstrated, that this effect is entirely caused by the residual stresses, which were not considered in the evaluation of the welded specimen data.

When a fatigue crack is propagating in a residual stress field, for example in a welded plate, the stress intensity at the crack front is influenced by the combined effect of residual stresses and the stress resulting from the externally applied (nominal) load. Within the validity limit of linear elasticity the total stress intensity factor acting at the crack tip is given by the sum of the residual stress and external loading contributions (superposition principle) [14]. The K value (= $K_{max} - K_{min}$) remains unaffected by K_{rs}, since the residual stress K_{rs} has to be added to the whole nominal or applied loading stress intensity range K. On the other hand the true load ratio $R_t = (K_{min}+K_{rs})/(K_{max}+K_{rs})$ differs from the applied load ratio R. In other words, residual stresses rise (tensile stresses) or lower (compressive stresses) the mean stress or load ratio R of the applied loading.

Compared to steel, da/dN-K curves of aluminum alloys are much more sensitive to load ratio effects, especially at low load levels and in the range of R < 0.5 [15]. For a given load K crack growth rates increase with increasing R. The reason for this behavior is that particularly at low or negative R-ratios only a part of the applied K, designated as the "effective stress intensity factor range K_{eff}", acts as driving force at the crack tip [16]. The underlying physical mechanisms of this effect are still being debated [17]. So far it is important to know, that K_{eff} is usually calculated from empirical relationships which depend on K and R [18].

Assuming that the real resistance against FCP of the welded specimens is equal to the parent material resistance, it is now possible to predict the constant amplitude da/dN-K curves of the welded specimens. For a given crack length and nominal load ratio the true load ratio R_t is calculated using the K_{rs} distribution of Figure 3. The effective stress intensity factor range K_{eff} of the welded specimens is obtained by inserting

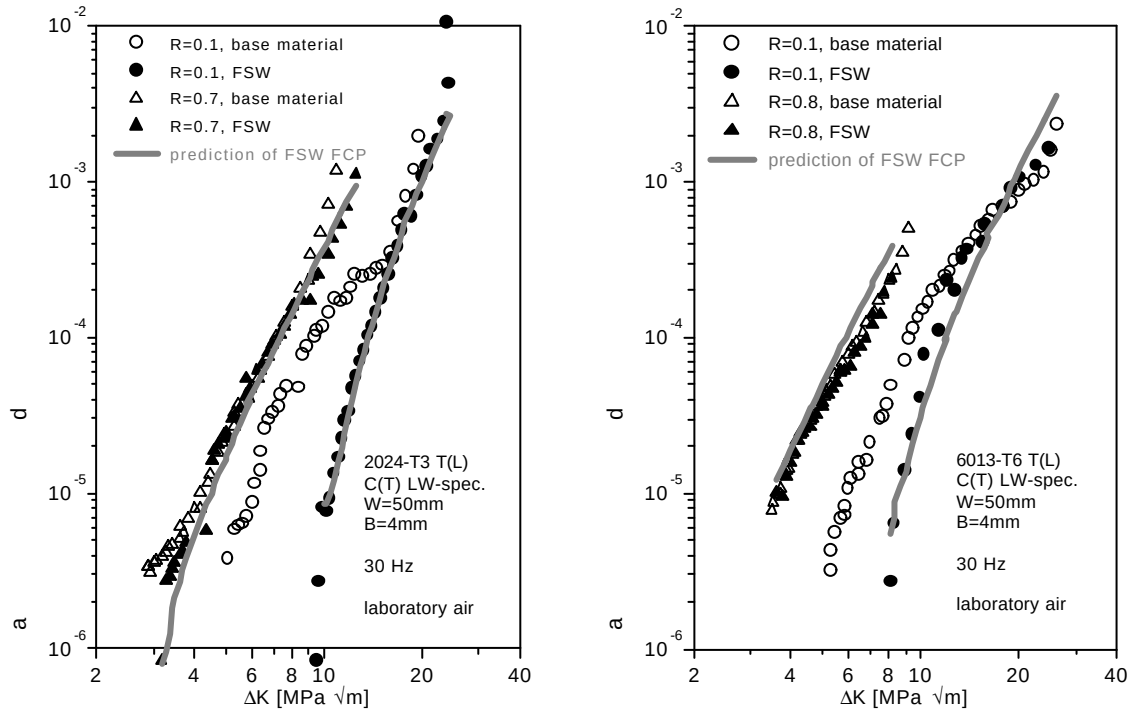

Figure 4: Fatigue crack propagation curves of longitudinal weld specimens compared to the base material data and the prediction.

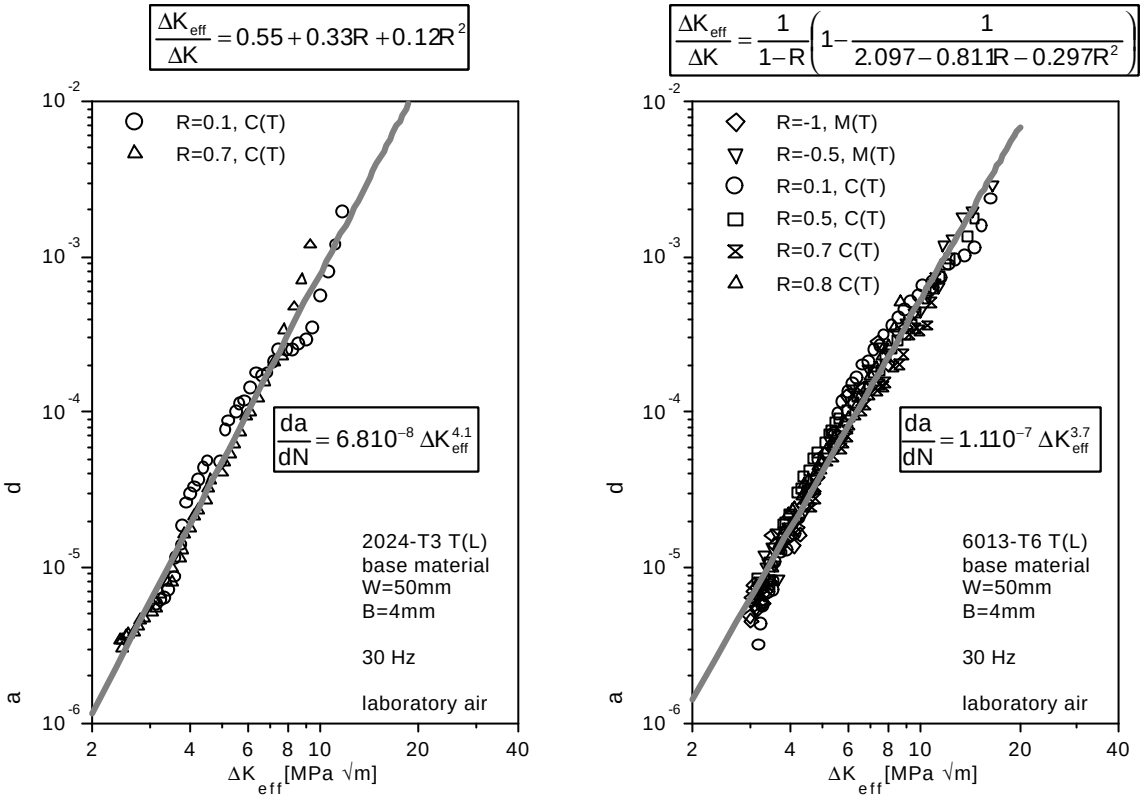

Figure 5: Effective parent material FCP curves fitted by power laws. K_{eff} was calculated by the empirical formulas on top of the figures taken from [18] (2024-T3) and [8] (6013-T6).

R_t in the K_{eff}-K-relationships given on top of Figure 5. The fatigue crack growth rate da/dN is then estimated by the simple power laws shown in Figure 5. The predicted FCP curves are very close to the data measured with the welded specimens, Figure 4. This means that our assumption was right and that the apparent improvement of FGP properties at low loads and load ratios displayed in Figure 4 is solely caused by compressive residual stresses present in the crack tip region of the C(T) specimens.

FCP IN TRANSVERSE WELD SPECIMENS

To get pronounced residual stress effects on da/dN it was essential to keep K and R constant at relatively low values (K < 15 MPa√m, R = 0.1) during the tests of the transverse weld (TW) C(T)-specimens. Because of the very low loads at the end of the tests (< 1 % of machine capacity), R and K deviated slightly from the constant values at a/W > 0.75. In Figure 6 the FSW fatigue crack propagation results of two TW specimens were therefore normalized with the respective fatigue crack propagation values of the parent material at the same nominal loading. The da/dN-prediction was calculated as described in the previous section. Also for this specimen geometry there is a favorable agreement between experimental and predicted values. This indicates that acceleration, deceleration and final acceleration of the crack crossing the weld is mainly caused by residual stresses and not by varying resistance to FCP of the different weld microstructures.

CONCLUSIONS

On the basis of the effective stress intensity factor range K_{eff}-approach and a simple residual stress intensity factor estimation it was shown that the differences in FCP behavior of welded specimens and parent material (2024-T3 and 6013-T6) are almost completely caused by residual stresses and not by the different resistance to FCP of the various weld microstructures.

ACKNOWLEDGEMENTS

The authors wish to thank Mr. U. Fuchs, and Mr. H.-W. Sauer for their support in welding and in the experimental investigations and Mr. F. Palm from the EADS Corporate Research Center, Munich, for kindly providing some of the FSW joints.

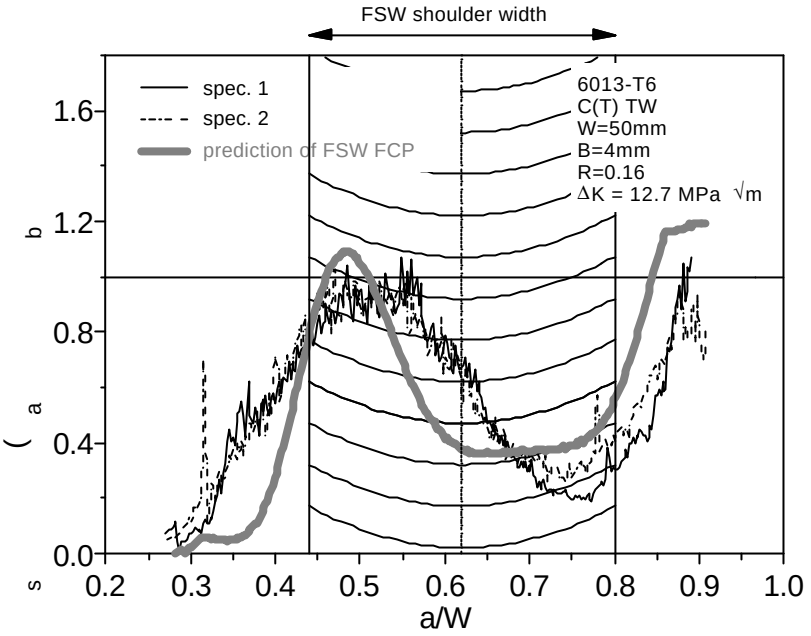

Figure 6: Fatigue crack propagation rates of TW specimens under constant K and R loading compared to the prediction using base material K_{eff} data and the K_{rs} distribution in the specimens.

REFERENCES

[1] Thomas, W.M. et al. (1992). *European Patent*, EP 0 615 480 B1.

[2] Haagensen, P.J., Midling, O.T. and Ranes, M. (1995). In: *2nd International Conference on Surface Treatment 95*, Vol. II, pp. 225-237.

[3] Dalle Donne, C. and Biallas, G. (1999). In: *European Conference on Spacecraft Structures, Materials and Mechanical Testing*, Stavrinidis, C., Rolfo, A. and Breitbach, E. (Eds.), ESA SP-428, pp. 309-314.

[4] Braun, R., Biallas, G., Dalle Donne, C. and Staniek, G. (1999). In: *Materials for Transportation Technology EUROMAT '99 - Vol. 1*, Winkler, P.J. (Ed.), Wiley-VCH, pp. 150-155.

[5] Biallas, G., Braun, G., Dalle Donne, C., Staniek, G. and Kaysser, W. (1999). In: *1st International Symposium on Friction Stir Welding*, TWI, UK, cd-rom.

[6] Bussu, G. and Irving, P. E. (1999). ibid.

[7] Hori, H., Makita, S. and Hino, H. (1999). ibid.

[8] Dalle Donne, C., Biallas, G., Ghidini, T. and Raimbeaux, G. (2000). In: *Second International Conference on Friction Stir Welding*, TWI, UK, cd-rom.

[9] Bachmann, V., Marci, G. and Sengebusch, P. (1994). In: *Automation in Fatigue and Fracture: Testing and Analysis, ASTM STP 1231*, Amzallag, G. (Ed.), ASTM, Philadelphia, 1994, pp. 146-163.

[10] Schindler, H.-J., Cheng, W. and Finnie, I. (1997) *Experimental Mechanics*, 37, pp. 272-277.

[11] Prime, M.B. (1999) *Fatigue Fract. Engn. Mater. Struct.*, 22, pp. 195-204.

[12] Schindler, H.-J. and Landolt, R. (1996). In: *Proc. of the 4th European Conference on Residual Stresses*, pp. 509-517.

[13] Ohta, A., Sasaki, E., Nihei, M., Kosuge, M. and Inagaki, M. (1982) *Int. J. Fatigue*, 4, pp. 233-237.

[14] Beghini, M. and Bertini, L. (1994) *Engng. Fracture Mech.*, 36, pp. 379-387.

[15] Bucci, R.J. (1996). In: *ASM Handbook Vol. 19, Fatigue and Fracture*, Lampman, S.R. (Ed.), ASM International, 1996, pp. 771-812.

[16] Elber, W. (1970) *Engng. Fracture Mech.*, 2, pp. 37-45.

[17] Lang, M. and Marci, G. (1999). In: *Fatigue and Fracture Mechanics: 29th Volume, ASTM STP 1332*, Panontin, L. and Sheppard, D.S. (Eds.), ASTM, 1999, pp. 474-495.

[18] Schijve, J. (1988). In: *Mechanics of Fatigue Crack Closure, ASTM STP 982*, Newman, J.C and Elber, W (Eds.), ASTM, Philadelphia, 1988, pp. 5-34.